

Formation of oxide phases in the system $\text{Fe}_2\text{O}_3\text{--Gd}_2\text{O}_3$

S. MUSIĆ, V. ILAKOVAC, M. RISTIĆ

Rudjer Bošković Institute, PO Box 1016, 41001 Zagreb, Croatia, Yugoslavia

S. POPOVIĆ

Physics Department, Faculty of Science, PO Box 162, 41001 Zagreb, Croatia, Yugoslavia

The formation of oxide phases in the system $(1 - x) \text{Fe}_2\text{O}_3 + x\text{Gd}_2\text{O}_3$ was investigated for $0 \leq x \leq 1$. On the basis of XRD measurements the distribution of oxide phases, $\alpha\text{-Fe}_2\text{O}_3$, $\text{Gd}_3\text{Fe}_5\text{O}_{12}$, GdFeO_3 and Gd_2O_3 was determined, as a function of x . No solid solutions were observed with certainty even at the very ends of the concentration range. This was also confirmed by ^{57}Fe Mössbauer spectroscopy. New accurate crystallographic data for $\text{Gd}_3\text{Fe}_5\text{O}_{12}$ are given. The formation of oxide phases in the system $\text{Fe}_2\text{O}_3\text{--Gd}_2\text{O}_3$ is compared with the data for analogous system $\text{Fe}_2\text{O}_3\text{--Eu}_2\text{O}_3$.

1. Introduction

In the last decade significant attention has been paid to the chemistry and physics of mixed oxides. These materials have already found applications in a great variety of technical fields. Generally, they exhibit specific electrical, magnetic, magneto-optical, piezoelectric and other physical properties. Mixed oxides can be prepared, for example, using coprecipitation, sol-gel procedure, solid state reactions, ceramic sintering, and film growth on different substrates. In our previous papers [1–4] we observed the relationships between the preparation of mixed oxides and the nature of metal cations on one hand and the chemical and structural properties of these oxides on the other hand.

The oxide system $\text{Fe}_2\text{O}_3\text{--R}_2\text{O}_3$, where R is yttrium or a rare-earth element, has been studied from different standpoints. Mössbauer spectroscopy is a particularly useful technique for the characterization of these oxide systems.

The orthoferrites, RFeO_3 , where R is yttrium or a rare-earth element, belong to the group of materials which exhibit weak ferromagnetism. A detailed Mössbauer studies on the rare-earth orthoferrites appeared in the 1960s [5–9]. ^{57}Fe Mössbauer spectra of rare-earth orthoferrites, RFeO_3 , show hyperfine magnetic splitting (one sextet of lines). The hyperfine magnetic field, extrapolated to 0 K, decreases regularly with the atomic number of R from 564 kOe ($1 \text{ Oe} = 79.58 \text{ A m}^{-1}$) for LaFeO_3 to 545.5 kOe for LuFeO_3 , and this effect can be ascribed to the changes of ionic radius of the rare-earth cation. The Néel temperature also decreases from 740 K for LaFeO_3 to 623 K for LuFeO_3 .

Yttrium and lanthanide garnets represent compounds of a significant practical importance. For instance, yttrium iron garnet (YIG) ceramics have found applications in microwave techniques. Sztanisław *et al.*

[10] investigated the formation and structural properties of YIG.

Eibshütz and Lines [11–13] measured the ^{57}Fe Mössbauer spectrum of amorphous $\alpha\text{-YIG}$ at 4.2 K. The second-order quadrupole shift, the sign distribution of electric field gradient (EFG) and the linewidth asymmetry of the hyperfine magnetic splitting spectrum at 4.2 K were discussed.

Nine garnets, $\text{R}_3\text{Fe}_5\text{O}_{12}$, $\text{R} = \text{Y, Sm, Eu, Gd, Tb, Dy, Ho, Er}$ or Tm , were investigated by Mössbauer spectroscopy at 590 K [14]. Regular changes of the quadrupole splitting value dependent on the radius of R^{3+} were found for a and d sublattices. The observed changes were ascribed to the increase of local lattice distortions with decreasing radius of the R^{3+} cation. The absolute Mössbauer absorption fractions for rare-earth garnets were calculated.

Mössbauer spectroscopy and magnetic measurements were applied in the study of Al-substituted YIG [15]. The formation of different oxide phases, such as $\alpha\text{-Fe}_2\text{O}_3$, YFeO_3 and $\text{Y}_3\text{Fe}_5\text{O}_{12}$ was observed during the preparation of YIG. Mössbauer spectra allowed a quantitative determination of incorporated Al^{3+} ions in the garnet structure. The values of the Curie temperature obtained by Mössbauer spectroscopy and magnetic measurements were in good agreement.

Substituted YIG or rare-earth garnets were also studied by other researchers [16–20] using Mössbauer spectroscopy as an experimental technique.

Rare-earth garnets play an important role in the development of magneto-optical devices [21, 22]. The magneto-optical phenomenon, also known as the Faraday effect, occurs when linearly polarized light is transmitted through a magnetic medium, and as a result of this process, the plane of polarization may rotate or become elliptical in dependence on the direction of magnetization. $\text{Y}_3\text{Fe}_5\text{O}_{12}$ garnet is generally used in long-distance optical communications at

wavelengths from 1.3 to 1.6 μm . Bi-substituted rare-earth garnets, $\text{Bi}_x\text{R}_{3-x}\text{Fe}_5\text{O}_{12}$, where R is a rare-earth element, are more promising materials for magneto-optical applications, due to a better ratio between the Faraday rotation coefficient, θ_F , for the wavelength of the light applied, and the absorption loss, α .

The aim of the present investigation is to obtain information about the phase composition and structural properties of different oxides formed in the system $\text{Fe}_2\text{O}_3\text{-Gd}_2\text{O}_3$. The correlation between this oxide system and the system $\text{Fe}_2\text{O}_3\text{-Eu}_2\text{O}_3$ is elaborated.

2. Experimental procedure

AR chemicals and bidistilled water were used for the preparation of the samples. The hydroxides, $\text{Fe}(\text{OH})_3/\text{Gd}(\text{OH})_3$, were coprecipitated by adding NH_4OH to corresponding $\text{Fe}(\text{NO}_3)_3 + \text{Gd}(\text{NO}_3)_3$ solutions. The coprecipitates were carefully washed and then dried. Samples S_0 to S_{12} were obtained by heating the corresponding hydroxides (coprecipitates) for 1 h at 200 $^\circ\text{C}$, for 1 h at 300 $^\circ\text{C}$, for 1 h at 500 $^\circ\text{C}$, for 1 h at 600 $^\circ\text{C}$ and for 4 h at 900 $^\circ\text{C}$ ("step-by-step" heating). The chemical composition of samples S_0 to S_{12} , prepared in the system $(1-x)\text{Fe}_2\text{O}_3 + x\text{Gd}_2\text{O}_3$, is given in Table I.

X-ray diffraction powder patterns were taken at room temperature using a counter diffractometer with monochromatized CuK_α radiation (Philips diffracto-

meter, proportional counter and graphite monochromator).

^{57}Fe Mössbauer spectra were recorded using a commercial Mössbauer spectrometer produced by Wissenschaftliche Elektronik GmbH. An Amersham $^{57}\text{Co-Rh}$ source was used. The standard absorbers, $\alpha\text{-Fe}$, $\alpha\text{-Fe}_2\text{O}_3$ and $^{57}\text{Fe-Rh}$, were also used.

3. Results and discussion

The oxide phases found in our samples, $\alpha\text{-Fe}_2\text{O}_3$, $\text{Gd}_3\text{Fe}_5\text{O}_{12}$, GdFeO_3 and Gd_2O_3 , were identified using the data contained in the Powder Diffraction File, JCPDS, [23]. Crystallographic data for these phases are given in Table II, together with the data for analogous phases existing in the system $\text{Fe}_2\text{O}_3\text{-Eu}_2\text{O}_3$, studied previously [3].

The results of X-ray diffraction phase analysis of samples, prepared in the system $\text{Fe}_2\text{O}_3\text{-Gd}_2\text{O}_3$, are given in Table III. Characteristic parts of X-ray powder diffraction patterns (samples S_2 , S_4 , S_7 , S_9 and S_{10}) are shown in Fig. 1. The present results are similar to those obtained for the system $\text{Fe}_2\text{O}_3\text{-Eu}_2\text{O}_3$ [3]. In both systems the samples were prepared at the same final temperature of heating, 900 $^\circ\text{C}$. The similarity between the results obtained for the systems $\text{Fe}_2\text{O}_3\text{-Gd}_2\text{O}_3$ and $\text{Fe}_2\text{O}_3\text{-Eu}_2\text{O}_3$ is obviously a consequence of similar ionic radii of Gd and Eu (0.094 nm for Gd^{3+} and 0.097 nm for Eu^{3+} ; the ionic radius of Fe^{3+} being 0.067 nm) and the same structural types of $\text{Ln}_3\text{Fe}_5\text{O}_{12}$, LnFeO_3 and Ln_2O_3 , $\text{Ln} = \text{Gd}$ or Eu , as shown in Table II. The molar fractions of oxide phases present in the systems $\text{Fe}_2\text{O}_3\text{-Gd}_2\text{O}_3$ and $\text{Fe}_2\text{O}_3\text{-Eu}_2\text{O}_3$, as a function of the Ln_2O_3 content, are shown in Fig. 2. These quantitative data were obtained by application of the doping method [25, 26].

The present results of X-ray diffraction analysis of the system $\text{Fe}_2\text{O}_3\text{-Gd}_2\text{O}_3$ can be summarized as follows.

The molar fraction of $\alpha\text{-Fe}_2\text{O}_3$ decreases continuously as the content of Gd increases. The fraction of the garnet-type ferrite, $\text{Gd}_3\text{Fe}_5\text{O}_{12}$, increases with the content of Gd, having a maximum at the Gd_2O_3 molar content of $\sim 0.30\text{-}0.40$ (samples S_7 and S_8) and then decreases with a further increase of the Gd content. Orthoferrite, GdFeO_3 , appears already at the Gd_2O_3 molar content of 0.01 (sample S_1). Its molar

TABLE I Chemical composition of the samples in the system $(1-x)\text{Fe}_2\text{O}_3 + x\text{Gd}_2\text{O}_3$

Sample	Molar fraction
S_0	Fe_2O_3
S_1	$0.99\text{ Fe}_2\text{O}_3 + 0.01\text{ Gd}_2\text{O}_3$
S_2	$0.97\text{ Fe}_2\text{O}_3 + 0.03\text{ Gd}_2\text{O}_3$
S_3	$0.95\text{ Fe}_2\text{O}_3 + 0.05\text{ Gd}_2\text{O}_3$
S_4	$0.90\text{ Fe}_2\text{O}_3 + 0.10\text{ Gd}_2\text{O}_3$
S_5	$0.85\text{ Fe}_2\text{O}_3 + 0.15\text{ Gd}_2\text{O}_3$
S_6	$0.80\text{ Fe}_2\text{O}_3 + 0.20\text{ Gd}_2\text{O}_3$
S_7	$0.70\text{ Fe}_2\text{O}_3 + 0.30\text{ Gd}_2\text{O}_3$
S_8	$0.68\text{ Fe}_2\text{O}_3 + 0.32\text{ Gd}_2\text{O}_3$
S_9	$0.50\text{ Fe}_2\text{O}_3 + 0.50\text{ Gd}_2\text{O}_3$
S_{10}	$0.30\text{ Fe}_2\text{O}_3 + 0.70\text{ Gd}_2\text{O}_3$
S_{11}	$0.10\text{ Fe}_2\text{O}_3 + 0.90\text{ Gd}_2\text{O}_3$
S_{12}	Gd_2O_3

TABLE II Crystallographic data (at room temperature) for phases existing in the system $\text{Fe}_2\text{O}_3\text{-Gd}_2\text{O}_3$ and $\text{Fe}_2\text{O}_3\text{-Eu}_2\text{O}_3$

JCPDS PDF [23] Card No.	Compound	Space group	Unit-cell parameters (nm)
13-534	$\alpha\text{-Fe}_2\text{O}_3$	$R\bar{3}c$ (167)	Hexagonal axes: $a = 0.50340$, $c = 1.3752$
13-327	$\text{Gd}_3\text{Fe}_5\text{O}_{12}$	$Ia\bar{3}d$ (230) [24]	$a = 1.2470$ [24]
23-1069	$\text{Eu}_3\text{Fe}_5\text{O}_{12}$	$Ia\bar{3}d$ (230)	$a = 1.2496$
15-196	GdFeO_3	$Pbnm$ (62)	$a = 0.5346$, $b = 0.5616$, $c = 0.7668$
8-407	EuFeO_3	$Pbnm$ (62)	$a = 0.5371$, $b = 0.5611$, $c = 0.7686$
12-797	Gd_2O_3	$Ia\bar{3}$ (206)	$a = 1.0813$
12-393	Eu_2O_3	$Ia\bar{3}$ (206)	$a = 1.0869$

TABLE III X-ray diffraction phase analysis of samples in the system $\text{Fe}_2\text{O}_3\text{-Gd}_2\text{O}_3$

Starting composition $\text{Fe}_2\text{O}_3\text{:Gd}_2\text{O}_3$ (molar ratio)	Phase composition as found by XRD (approximate molar fractions)			
	$\alpha\text{-Fe}_2\text{O}_3$	$\text{Gd}_3\text{Fe}_5\text{O}_{12}$	GdFeO_3	Gd_2O_3
Fe_2O_3	1			
99:1	0.98		0.02	
97:3	0.92	0.01	0.07	
95:5	0.85	0.05	0.10	
90:10	0.70	0.18	0.12	
85:15	0.45	0.40	0.15	
80:20	0.30	0.65	0.05	
70:30	0.06	0.90	0.04	
68:32	0.06	0.90	0.04	
50:50		0.20	0.70	0.10
30:70		0.05	0.45	0.50
10:90		0.02	0.08	0.90
Gd_2O_3				1

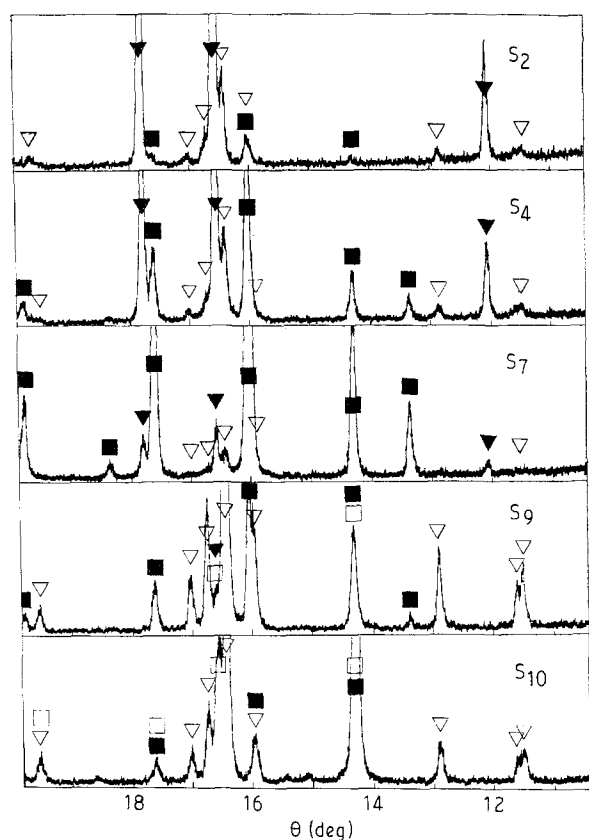


Figure 1 Characteristic parts of X-ray diffraction powder patterns of several samples in the system $\text{Fe}_2\text{O}_3\text{-Gd}_2\text{O}_3$ (radiation: monochromatized $\text{CuK}\alpha$). (S_2 3 mol % Gd_2O_3 , S_4 10 mol % Gd_2O_3 , S_7 30 mol % Gd_2O_3 , S_9 50 mol % Gd_2O_3 , S_{10} 70 mol % Gd_2O_3) (∇ $\alpha\text{-Fe}_2\text{O}_3$, \blacksquare $\text{Gd}_3\text{Fe}_5\text{O}_{12}$, \triangle GdFeO_3 , \square Gd_2O_3)

fraction slowly increases with the Gd content, having a small maximum at ~ 0.15 (sample S_5) and a pronounced maximum at ~ 0.50 (sample S_9), i.e. at the starting molar ratio $\text{Fe}_2\text{O}_3\text{:Gd}_2\text{O}_3 = 1:1$. The fraction of GdFeO_3 decreases as the Gd content increases above 0.50. The phase Gd_2O_3 appears at the starting composition $\text{Fe}_2\text{O}_3\text{:Gd}_2\text{O}_3 = 1:1$ (sample S_9), and its fraction increases with the Gd content.

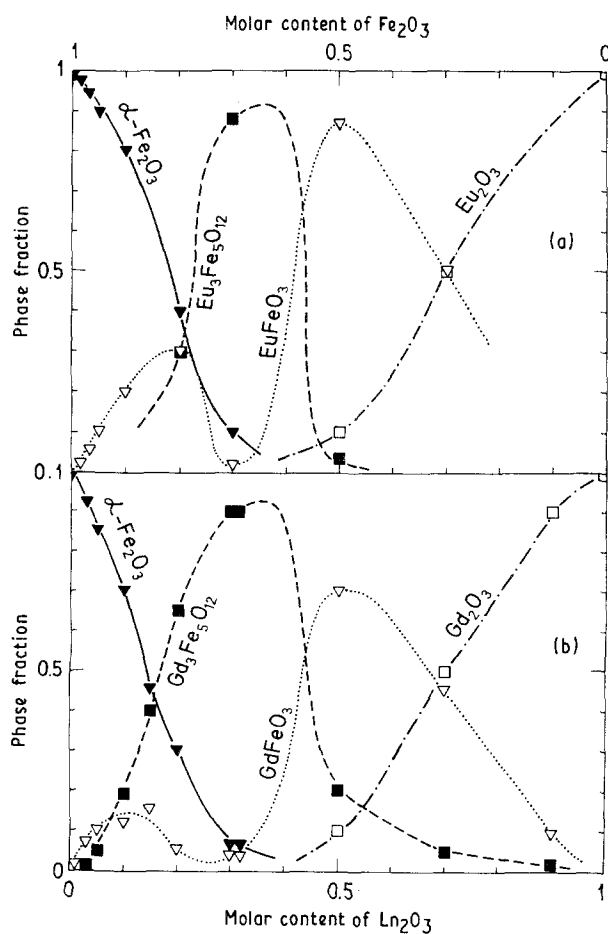


Figure 2 Distribution of oxide phases (molar fractions) present in the systems (a) $\text{Fe}_2\text{O}_3\text{-Eu}_2\text{O}_3$ and (b) $\text{Fe}_2\text{O}_3\text{-Gd}_2\text{O}_3$ (Fig. 2b), as a function of the molar content of Ln_2O_3 .

All oxide phases present in samples $\text{Fe}_2\text{O}_3\text{-Ln}_2\text{O}_3$, $\text{Ln} = \text{Gd}$ or Eu , prepared at the final temperature of 900°C , are well crystallized showing sharp X-ray diffraction lines, which are well resolved in the spectral components $K_{\alpha_1\alpha_2}$ at higher Bragg angles.

According to X-ray diffraction analysis the solid solutions were not formed in the system

TABLE IV Powder diffractometer data for $\text{Gd}_3\text{Fe}_5\text{O}_{12}$ (room temperature, radiation $\text{CuK}\alpha_1$, $\alpha\text{-Fe}_2\text{O}_3$ as internal standard) $a = (1.2460 \pm 0.0008)$ nm, space group $\text{Ia}\bar{3}d$ (230)

d_{obs} (nm)	d_{calc} (nm)	hkl	I/I_0
0.508	0.509	211	18
0.440	0.441	220	4
0.333	0.3330	321	12
0.311	0.3115	400	30
0.279	0.2786	420	100
0.2545	0.2543	422	40
0.2445	0.2444	510	3
		431	
0.2275	0.2275	521	14
0.2200	0.2203	440	5
0.2020	0.2021	611	12
		532	
0.1835	0.1837	631	4
0.1795	0.1798	444	15
0.1725	0.1728	640	35
0.1695	0.1696	721	10
		633 +	
0.1663	0.1665	642	38
0.1580	0.1582	732	3
		651	
0.1559	0.1558	800	12
0.1392	0.1392	840	9
0.1359	0.1359	842	20
0.1343	0.1344	921	2
		761 +	
0.1328	0.1328	664	7
0.1285	0.1285	932	2
		763	
0.1222	0.1222	10, 2, 0	3
		862	
0.1187	0.1188	10, 3, 1	4
		952 +	
0.1157	0.1157	10, 4, 0	15
		864	
0.1139	0.1137	10, 4, 2	7
0.1110	0.1110	11, 2, 1	3
		10, 5, 1 +	
0.1102	0.1101	880	10
0.1025	0.1024	12, 2, 0	5
0.1010	0.1011	12, 2, 2	8
		10, 6, 4	
0.09670	0.09671	11, 6, 3	2
		992 +	
0.09395	0.09392	12, 4, 4	5
0.09290	0.09287	12, 6, 0	15
		10, 8, 4	
0.09237	0.09236	13, 3, 2	2
		11, 6, 5 +	
0.09185	0.09186	12, 6, 2	5
0.08995	0.08992	888	5

+ Additional indices are possible.

$\text{Fe}_2\text{O}_3\text{-Gd}_2\text{O}_3$, as it was also concluded for the system $\text{Fe}_2\text{O}_3\text{-Eu}_2\text{O}_3$ [3]. The exception might be the far Gd_2O_3 -rich side (sample S_{11}). There is, however, no evidence (based on X-ray diffraction), which would support this assumption, except for the estimated molar fractions present in the sample S_{11} (Table III).

In the present work the powder diffraction data for $\text{Gd}_3\text{Fe}_5\text{O}_{12}$ contained in Reference 23 were improved. Accurate unit-cell parameters and interplanar

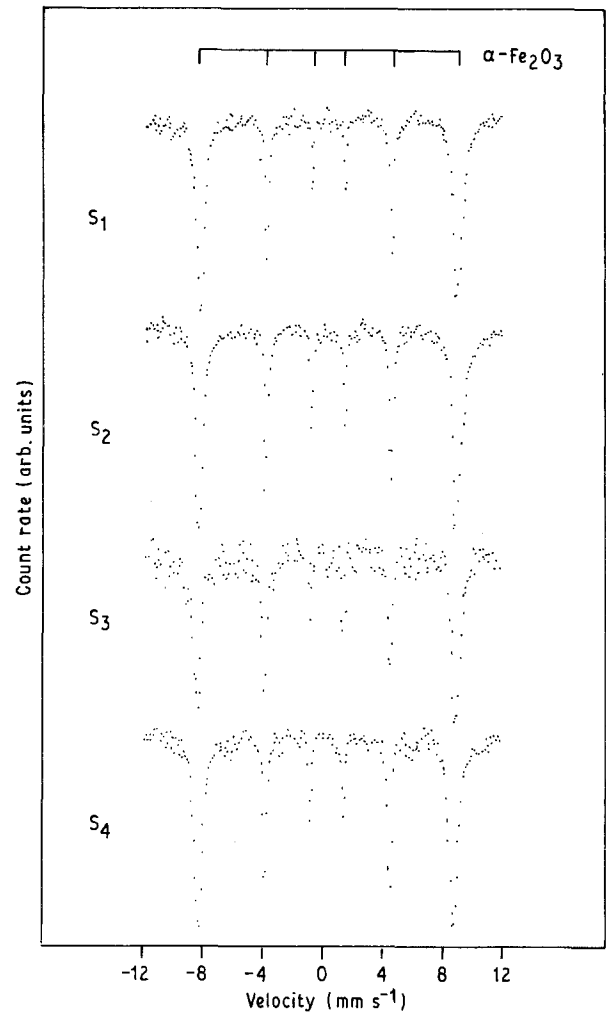


Figure 3 ^{57}Fe Mössbauer spectra of samples S_1 to S_4 recorded at room temperature.

spacings were obtained using $\alpha\text{-Fe}_2\text{O}_3$, already present in our samples, as internal standard. The new crystallographic data are listed in Table IV.

Figs 3 and 4 show the ^{57}Fe Mössbauer spectra of samples S_1 to S_7 , S_9 and S_{10} recorded at room temperature. The hyperfine magnetic field (HMF) of $\alpha\text{-Fe}_2\text{O}_3$ component for samples S_1 to S_4 has the same value (517 ± 1 kOe), as for the standard $\alpha\text{-Fe}_2\text{O}_3$ sample, S_0 . For sample S_5 the HMF value of $\alpha\text{-Fe}_2\text{O}_3$ component is slightly decreased to 515 ± 2 kOe. This result indicates that there is practically no Gd^{3+} dissolution into the $\alpha\text{-Fe}_2\text{O}_3$ structure at given experimental conditions, which is in agreement with the X-ray diffraction results. Generally, it is known that dissolution of metal ions into the $\alpha\text{-Fe}_2\text{O}_3$ structure decreases significantly the value of hyperfine magnetic field at ^{57}Fe nucleus.

The ^{57}Fe Mössbauer spectrum of sample S_7 indicates that $\text{Gd}_3\text{Fe}_5\text{O}_{12}$ is the dominant component in this sample. With a further increase of Gd content the spectral lines corresponding to GdFeO_3 start to be dominant. In sample S_{10} the HMF value of 500 ± 2 kOe was measured, which is in agreement with HMF value for GdFeO_3 (502 kOe at 296 K) obtained by Eibshütz *et al.* [7].

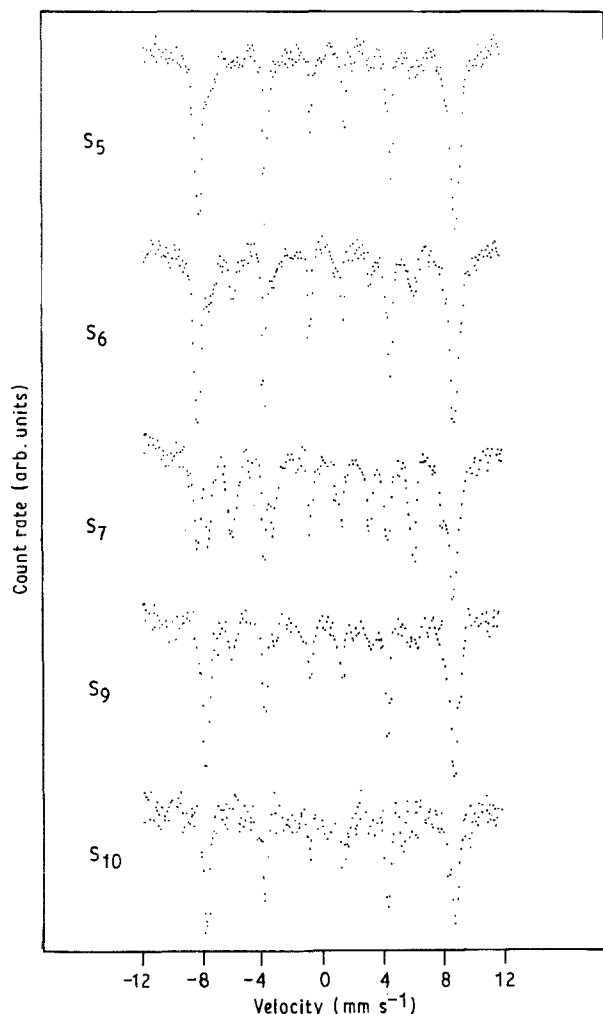


Figure 4 ^{57}Fe Mössbauer spectra of samples S_5 to S_7 , S_9 and S_{10} , recorded at room temperature.

References

1. S. MUSIĆ, S. POPOVIĆ and M. RISTIĆ, *J. Mater. Sci.* **24** (1989) 2722.
2. M. RISTIĆ, S. POPOVIĆ, M. TONKOVIĆ and S. MUSIĆ, *ibid.* in press.

3. M. RISTIĆ, S. POPOVIĆ and S. MUSIĆ, *J. Mater. Sci. Lett.* **9** (1990) 872.
4. S. MUSIĆ, S. POPOVIĆ, M. METIKOŠ-HUKOVIĆ and V. GVOZDIĆ, *ibid.* **10** (1991) 197.
5. M. EIBSHÜTZ, G. GORODETSKY, S. SHTRIKMAN and D. TREVES, *J. Appl. Phys.* **35** (1964) 1071.
6. D. TREVES, *ibid.* **36** (1965) 1033.
7. M. EIBSHÜTZ, S. SHTRIKMAN and D. TREVES, *Phys. Rev.* **156** (1967) 562.
8. J. M. D. COEY, G. A. SAWATZKY and A. H. MORRISH, *Phys. Rev.* **184** (1969) 334.
9. L. M. LEVINSON, M. LUBAN and S. SHTRIKMAN, *ibid.* **177** (1969) 864.
10. A. SZTANISLÁV, E. STERK, L. FETTER, M. FARKAS-JAHNKE and J. LÁBÁR, *J. Magn. Magn. Mater.* **41** (1984) 75.
11. M. EIBSHÜTZ and M. E. LINES, *Phys. Rev. B* **25** (1982) 4256.
12. M. E. LINES and M. EIBSHÜTZ, *ibid.* **25** (1982) 6042.
13. M. EIBSHÜTZ and M. E. LINES, *ibid.* **26** (1982) 2288.
14. V. N. BELOGUROV and V. A. BILINKIN, *Phys. Status Solidi a*, **63** (1981) 45.
15. C. MICHALK and W. THIEL, *ibid.* **90** (1985) 325.
16. A. P. DODOKIN and I. S. LYUBUTIN, *J. Physique* **40** (1979) C2-342.
17. I. S. LYUBUTIN, B. V. MILL, R. I. CHALABOV and A. V. BUTASHIN, *J. Phys. Chem. Solids* **46** (1985) 363.
18. Z. M. STADNIK and B. F. OTTERLOO, *J. Solid State Chem.* **48** (1983) 133.
19. Z. M. STADNIK, *J. Magn. Magn. Mater.* **37** (1983) 138.
20. K. SANEYOSHI, T. TORIYAMA, J. ITOH, K. HISATAKE and S. CHIKAZUMI, *ibid.* **31-34** (1983) 705.
21. J. F. DILLON, Jr., *ibid.* **84** (1990) 213.
22. N. KOSHIZUKA and T. OKUDA, *IEEE Trans. J. Magn. TJM-1* (1985) 1044.
23. International Centre for Diffraction Data, Joint Committee on Powder Diffraction Standards, 1601 Park Line, Swarthmore, PA 19081, USA.
24. J. E. WEIDENBORNER, *Acta Crystallogr.* **14** (1961) 1051.
25. S. POPOVIĆ and B. GRŽETA-PLENKOVIĆ, *J. Appl. Crystallogr.* **12** (1979) 205.
26. S. POPOVIĆ, B. GRŽETA-PLENKOVIĆ and T. BABIĆ-ŽUNIĆ, *ibid.* **16** (1983) 505.

Received 19 October 1990
and accepted 25 March 1991